Electronic- and crystal-structure effects on superconductivity in the $BaPb_{1-x}Bi_xO_3$ system

L. F. Mattheiss and D. R. Hamann
Bell Laboratories, Murray Hill, New Jersey 07974
(Received 19 March 1982; revised manuscript received 24 May 1982)

Self-consistent, scalar-relativistic, linear-augmented-plane-wave electronic-structure calculations have been carried out for the $BaPb_{1-x}Bi_xO_3$ system in the cubic ($x=0$, 0.3, 1) and body-centered-tetragonal ($x=0.3$) phases. The results suggest that the relatively high superconducting transition temperatures ($T_c \approx 13$ K) that are observed for $0.05 \leq x \leq 0.3$ are due to strong electron-phonon coupling which arises from modulation of the dominant ($sp\sigma$) interaction between neighboring Pb-Bi $6s$ and O $2p$ orbitals at E_F.

The discovery of high-temperature superconductivity in the perovskite-type $BaPb_{1-x}Bi_xO_3$ system for $0.05 \leq x \leq 0.3$ by Sleight *et al.*[1] in 1975 has led to subsequent and continuing investigations of the superconducting,[2,5–12] structural,[3,5] transport,[4,7–9] and calorimetric[11] properties of these materials. In particular, Sleight *et al.*[1] found that samples with $x \leq 0.3$ were black and metallic while those with higher values of x were bronze and semiconducting, with an activation energy of about 0.2 eV. The observed superconducting transitions were broad, with onset temperatures increasing from about $T_c=9$ K at $x=0.05$ to $T_c=13$ K for $x=0.3$.

In general, the results of subsequent investigations[2–12] on the $BaPb_{1-x}Bi_xO_3$ system have confirmed the main features of this initial study. Perhaps the most important new information on this system has been provided by the structural studies of Cox and Sleight.[3(b)] These studies show that the room-temperature crystal structure of these materials varies from orthorhombic → tetragonal → orthorhombic → monoclinic as a function of increasing x and superconductivity is confined to the tetragonal phase. A second interesting phenomenon is exhibited by the specific-heat data of Methfessel *et al.*[11] for samples with $x=0.25$. The standard C/T vs T^2 plot of these data contain no indication of a bulk specific-heat anomaly at the superconducting transition temperature and exhibit a finite intercept at $T=0$ that corresponds to an electronic contribution $\gamma=0.15$ mJ/(g atom K^2).

The trend from metallic-to-semiconducting behavior for increasing x has prompted considerable speculation regarding the electronic structure of these $BaPb_{1-x}Bi_xO_3$ compounds. Most ideas are based on the original proposal by Sleight *et al.*[1] in which a partially filled $Pb_{1-x}Bi_x$ $6s$ band overlaps the filled O $2p$ bands. This model assumes that the $6s$ band narrows and splits with increasing x, gradually leading to semiconducting behavior for $x \geq 0.35$. A more detailed model for explaining this semiconductor-metal transition has been proposed recently by Rice and Sneddon.[13] It involves a real-space pairing of electrons at the Bi sites for the Bi-rich compounds with $x \geq 0.35$ and a transition to a metallic-superconducting phase for $x \leq 0.35$ where Pb substitution dilutes the Bi lattice.

The purpose of the present investigation is to determine from first principles the electronic structure of these $BaPb_{1-x}Bi_xO_3$ compounds and to relate these results to the occurrence of high-temperature superconductivity. The calculations utilize a self-consistent, scalar-relativistic version of the linear-augmented-plane-wave (LAPW) method[14] in which the charge density and potential are treated in a completely general functional form and exchange-correlation effects are included in the local-density approximation using the Wigner interpolation formula.[15] For nonintegral values of x, the calculations incorporate the virtual-crystal approximation[16] (i.e., replace the $Pb_{1-x}Bi_x$ distribution by an average atom with atomic number $82+x$). This approximation provides, for intermediate values of x, a smooth interpolation between the extremely similar energy-band results for cubic $BaPbO_3$ and $BaBiO_3$.

The calculations have been carried out for the cubic modifications of $BaPbO_3$, $BaPb_{0.7}Bi_{0.3}O_3$, and $BaBiO_3$ (space group O_h^1) and the observed[3(b)] body-centered-tetragonal (bct) phase of $BaPb_{0.7}Bi_{0.3}O_3$ (space group D_{4h}^{18}). The cubic structure consists of a simple-cubic lattice of Ba with a Pb or Bi at the body center and O's at each face center. The bct structure is identical with that observed[17] in $SrTiO_3$ below 110 K. With the origin of coordinates at a Ti (or $Pb_{1-x}Bi_x$) site, this tetragonal distortion in $SrTiO_3$ results from a soft triply degenerate zone-boundary optic phonon with $R_{15'}$ symmetry.[18] The normal modes of this $R_{15'}$ phonon involve oxygen-atom displacements that correspond dynamically to rigid rotations of the TiO_3 (or $Pb_{1-x}Bi_xO_3$) octahedra about the three coordinate axes.[19] At the cubic-to-tetragonal transition, one of these modes is "frozen

 ©1982 The American Physical Society

in" and this produces a bct structure containing two formula units per cell in which neighboring octahedra are statically rotated about [001] by angles $\pm\phi$ of about 2° and 8° in $SrTiO_3$ and $BaPb_{0.7}Bi_{0.3}O_3$, respectively.

The LAPW energy bands for simple cubic $BaPb_{0.7}Bi_{0.3}O_3$ are plotted along symmetry lines in the Brillouin zone (BZ) in Fig. 1. The lowest set of core-like levels centered near −11.5 eV corresponds to the Ba $5p$ states whereas the unoccupied bands above 3.5 eV are predominantly Ba $5d$ states. The more tightly bound $Pb_{0.7}Bi_{0.3}$ $5d$ and O $2s$ states (which are not shown) form a broad (~5 eV) strongly admixed manifold centered near −17.5 eV. The remaining bands, extending from −11 to 5 eV, originate from the $Pb_{0.7}Bi_{0.3}$ $6s$ and O $2p$ states.

Despite its 16-eV bandwidth, this ten-band complex of O $2p$ and $Pb_{0.7}Bi_{0.3}$ $6s$ states can be interpreted in terms of a simple tight-binding model. This model involves three parameters, including the orbital energies $E_{2p}=-1.9$ eV, $E_{6s}=-4.1$ eV, and the nearest-neighbor two-center integral $(sp\sigma)=2.2$ eV. The O $2p$ orbitals at each site in the cubic phase are either parallel or perpendicular to the $O-Pb_{1-x}Bi_x$ bond directions. We represent these by $p_\parallel$ and $p_\perp$, respectively. The strong $(sp\sigma)$ interaction couples only the $Pb_{1-x}Bi_x$ $6s$ and O $2p_\parallel$ orbitals and this produces a pair of broad bands that extend from the R_1 state at −11 eV to the corresponding state at +5 eV. Because of translational symmetry, the states at X, M, and R involve two, four, and six nearest-neighbor s-p bonds, respectively. The roughly constant ~2-eV energy difference between the filled and empty X_1, M_1, and R_1 states is a signature of their tight-binding character.

The remaining cluster of narrow bands distributed below $E_{2p}=-1.9$ eV corresponds to the nonbonding O $2p_\perp$ orbitals. (These are completely flat in the simple model.) As indicated, the Fermi energy E_F falls about 1 eV above the top of these nonbonding states, within the broad $6s$-$2p_\parallel$ manifold. Relative to E_{2p}, the $Pb_{1-x}Bi_x$ $6s$ orbital energy $E_{6s}\approx E(\Gamma_1)$ decreases monotonically from −1.3 eV in cubic $BaPbO_3$ to −4.3 eV in $BaBiO_3$, thereby predicting $6s$-$2p$ overlap and metallic properties for all x in the simple-cubic phase. The fact that the 16-eV bandwidth of the $6s$-$2p_\parallel$ manifold is much greater than $\Delta E_{6s}=3$ eV lends further support to the virtual-crystal model for these alloys. It is clear that a more sophisticated technique for treating the random potential (such as the coherent-potential approximation[16]) will not give significant localized density-of-states (DOS) differences on the Pb and Bi for these values.

DOS curves for the cubic and bct phases of $BaPb_{0.7}Bi_{0.3}O_3$ are show in in Figs. 2(a) and 2(b), respectively. These results have been obtained using the tetrahedral method and LAPW eigenvalues calculated on a uniform mesh containing 84 (100) points in the irreducible wedge of the cubic (bct) BZ. For the cubic calculations, this mesh corresponds to seven points along the ΓX line or 1728 points in the entire BZ. Essentially, the same mesh points were chosen for the bct DOS calculation (864 total points in the BZ).

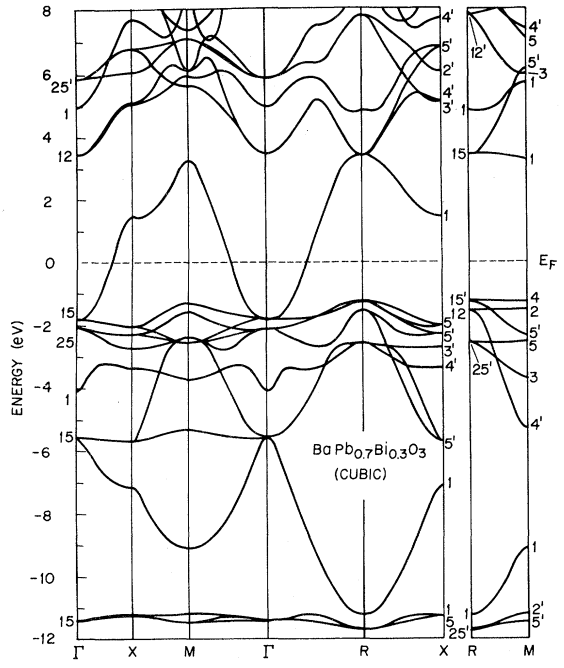

FIG. 1. LAPW energy bands for cubic $BaPb_{0.7}Bi_{0.3}O_3$ along symmetry lines in the Brillouin zone.

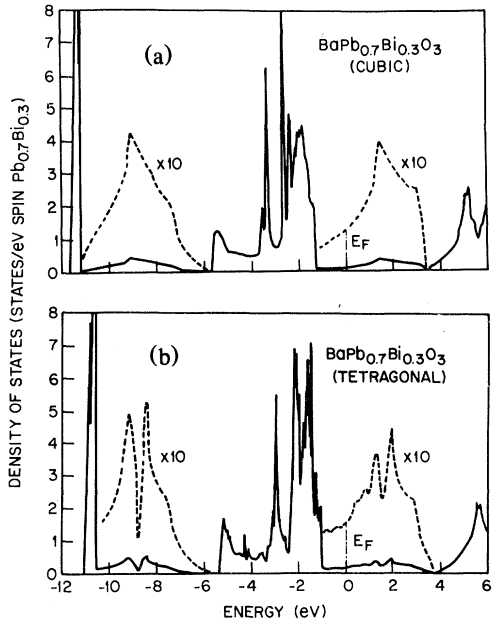

FIG. 2. Density-of-states curves for (a) cubic and (b) body-centered-tetragonal $BaPb_{0.7}Bi_{0.3}O_3$.

Various features such as shoulders and peaks in the cubic DOS curves in Fig. 2(a) are readily associated with specific energy-band features in Fig. 1. The main difference between the cubic and bct DOS curves is the presence of additional structure in the latter results and the occasional splitting of cubic DOS peaks. This is not surprising since the bct bands are essentially a remapped version of the simple-cubic results in which the R point is folded into the BZ center Γ.

Convergence tests have shown that the small $\sim$0.3-eV difference in the position of the initial DOS peak below E_F in Figs. 2(a) and 2(b) is due to limitations in the LAPW basis-function size in the latter bct calculation. This causes a lowering of the $Pb_{0.7}Bi_{0.3}$ $6s$ band (and E_F) relative to the nonbonding O $2p_\perp$ states in Fig. 2(b).

The calculated value for the $x=0.3$ bct DOS at E_F is 0.16, in units "states/eV spin $Pb_{0.7}Bi_{0.3}$ atom." The measured[11] $T=0$ specific-heat γ for $BaPb_{0.75}Bi_{0.25}O_3$ corresponds to 0.03 in these units. A rigid-band interpolation to $x=0.25$ yields a value of 0.15. If we assume that this calculated value is accurate and neglect phonon-enhancement effects, then we can estimate that approximately 80% of the two measured samples was in the superconducting phase.

This combination of a nearly spherical Fermi surface and a low DOS at E_F makes these $BaPb_{1-x}Bi_xO_3$ compounds rather unlikely prospects for high-temperature superconductivity. For example, our band DOS value of 0.16 is only about 60% that of Pb ($T_c=7.2$ K). However, several important keys for solving this puzzle are provided by structural features of the bct, orthorhombic, and monoclinic phases. The first is the fact that the primitive cell for each distorted phase contains two formula units. More importantly, the corresponding BZ's are each geometrically similar to that for an fcc lattice (i.e., one in which "superlattice" effects cause the simple-cubic R point to be remapped into the BZ center Γ). In simplest terms, this can be viewed as the formation of a rocksalt-type lattice of Pb-Bi atoms with inequivalent nearest neighbors.

Neglecting this inequivalence, the extension of our tight-binding model to this geometry provides a convincing explanation for both the stability of the monoclinic phase near $x=1$ and the observed semiconducting behavior at $x=1$. In particular, this model predicts the perfect nesting of identical electron and hole Fermi-surface sheets for $x=1$. In this situation, an infinitesimal distortion is expected to open a semiconductor gap and stabilize the distortion.

Preliminary studies which extend this model to incorporate characteristic distortions of the bct and monoclinic phases have been carried out. The former case is straightforward since it involves rigid rotations of octahedra with negligible changes in $Pb_{1-x}Bi_x$–O bond distances. This distortion produces small ($\sim$0.01 eV) and incomplete splittings which only partially remove the nesting degeneracies at E_F for $x=1$. Thus a bct distortion will not produce a semiconducting gap. Nevertheless, these splittings are reflected in the bct DOS curve in Fig. 2 as minima at energies 1.5 and -8.8 eV, respectively.

Analogous model studies demonstrate that a finite gap is opened when simple-cubic $BaBiO_3$ is distorted in such a way to produce a rocksalt-type lattice of inequivalent BiO_6 octahedra with different Bi-O bond distances (i.e., a cubic analog of the monoclinic structure). Although an accurate determination of the distance dependence of the $(sp\sigma)$ interaction awaits the completion and analysis of LAPW calculations for monoclinic $BaBiO_3$, these preliminary model studies indicate large splittings of these nesting degeneracies near the BZ boundary, corresponding to deformation potentials of $\sim$6 (eV/Å). These decrease rapidly as one moves toward Γ and correspond to $\sim$1 (eV/Å) at E_F for $x\approx 0.3$. Analogous calculations for ferroelectric-type displacements of $Pb_{1-x}Bi_x$ atoms yield deformation potentials which are a maximum [$\sim$1 (eV/Å)] at Γ and then decrease rapidly.

In conclusion, we see that the band structure for $BaPb_{1-x}Bi_xO_3$ contains the elements necessary to understand the superconductivity of these materials and the semiconducting phase at $x=1$. The phonon modes important for superconductivity are likely to involve "ferroelectric" displacements of the Pb-Bi atoms and "breathing-mode" displacements of the O atoms. The structural phase transitions from the reference cubic phase to the observed sequence of structures all involve the "freezing in" of various R-point phonon modes. At present, the small total-energy difference involved in the bct distortion is probably not amenable to calculation. However, the model $6s$-$2p$ band structure does provide a strong Fermi-surface instability to explain the terminal ($x=1$) structural transition and its semiconducting character.

The semiconductivity of the $0.35<x<1$ materials is not easily understood in terms of a band picture. This supposedly orthorhombic phase is the least well characterized structure[3(b)] and we must entertain the possibility of a mixed phase or a finite defect concentration which could shift E_F. With the future availability of single-crystal samples, it is important that photoemission and optical studies be carried out to test the global features of the band structure presented here, particularly the placement of E_F.

ACKNOWLEDGMENTS

We are particularly pleased to acknowledge very useful and stimulating conversations with W. Weber, W. W. Warren, Jr., T. M. Rice, L. Sneddon, B. Batlogg, G. K. Wertheim, D. Cox, and C. E. Methfessel on various aspects of this investigation.

[1]A. W. Sleight, J. L. Gillson, and P. E. Bierstedt, Solid State Commun. 17, 27 (1975).
[2]C. W. Chu, S. Huang, and A. W. Sleight, Solid State Commun. 18, 977 (1976).
[3](a) D. E. Cox and A. W. Sleight, Solid State Commun. 19, 969 (1976); (b) in *Proceedings of Conference on Neutron Scattering, Gatlinburg, Tennessee, 1976,* edited by R. M. Moon (National Technical Information Service, Springfield, Va., 1976); (c) Acta Crystallogr. Sect. B 35, 1 (1979).
[4]J. B. Clark, F. Dachille, and R. Roy, Solid State Commun. 19, 989 (1976).
[5]Y. Khan, K. Nahm, M. Rosenberg, and H. Willner, Phys. Status Solidi A 39, 79 (1977).
[6]L. R. Gilbert, R. Messier, and R. Roy, Thin Solid Films 54, 129 (1978).
[7]E. A. Protasov, S. V. Zaitsev-Zotov, Y. N. Venevtsev, and V. V. Bogatko, Fiz. Tverd. Tela. (Leningrad) 20, 3503 (1978) [Sov. Phys. Solid State 20, 2028 (1978)].
[8]M. Suzuki, T. Murakami, and T. Inamura, Jpn. J. Appl. Phys. 19, L72 (1980).
[9]T. D. Thanh, A. Koma, and S. Tanaka, Appl. Phys. 22, 205 (1980).
[10]V. V. Bogatko and Yu. N. Venevtsev, Fiz. Tverd. Tela. (Leningrad) 22, 1211 (1980) [Sov. Phys. Solid State 22, 705 (1980)].
[11]C. E. Methfessel, G. R. Stewart, B. T. Matthias, and C. K. N. Patel, Proc. Nat. Acad. Sci. U.S.A. 77, 6307 (1980).
[12]M. K. Wu, R. L. Meng, S. Z. Huang, and C. W. Chu, Phys. Rev. B 24, 4075 (1981).
[13]T. M. Rice and L. Sneddon, Phys. Rev. Lett. 47, 689 (1981).
[14]O. K. Andersen, Phys. Rev. B 12, 3060 (1975).
[15]E. Wigner, Phys. Rev. 46, 1002 (1934).
[16]H. Ehrenreich and L. M. Schwartz, in *Solid State Physics,* edited by H. Ehrenreich, F. Seitz, and D. Turnbull (Academic, New York, 1976), Vol 31.
[17]H. Unoki and T. Sakudo, J. Phys. Soc. Jpn. 23, 546 (1967).
[18]P. A. Fleury, J. F. Scott, and J. M. Worlock, Phys. Rev. Lett. 21, 16 (1968).
[19]R. A. Cowley, Phys. Rev. 134, A981 (1964). We point out that Cowley's origin of coordinates is at the Sr site and the present symmetry designation of the R_{15}, phonon thereby changes to R_{25}.